Physics Letters B 682 (2009) 291–296

Contents lists available at ScienceDirect

Physics Letters B

www.elsevier.com/locate/physletb

Discovering the Higgs bosons of minimal supersymmetry with bottom quarks

Chung Kao *, Shankar Sachithanandam, Joshua Sayre, Yili Wang

Homer L. Dodge Department of Physics and Astronomy, University of Oklahoma, Norman, OK 73019, USA

ARTICLE INFO

Article history:
Received 9 August 2009
Received in revised form 27 October 2009
Accepted 30 October 2009
Available online 13 November 2009
Editor: M. Cvetič

PACS:
14.80.Cp
14.80.Ly
12.60.Jv
13.85.Qk

ABSTRACT

We investigate the prospects for the discovery of a neutral Higgs boson produced with one bottom quark followed by Higgs decay into a pair of bottom quarks at the CERN Large Hadron Collider (LHC) and the Fermilab Tevatron Collider. We work within the framework of the minimal supersymmetric standard model. The dominant physics background is calculated with realistic acceptance cuts and efficiencies including the production of $bb\bar{b}$, $\bar{b}b\bar{b}$, $jb\bar{b}$ ($j = g, q, \bar{q}$; $q = u, d, s, c$), $t\bar{t} \to b\bar{b}jj\ell\nu$, and $t\bar{t} \to b\bar{b}jjjj$. Promising results are found for the CP-odd pseudoscalar (A^0) and the heavier CP-even scalar (H^0) Higgs bosons with masses up to 800 GeV for the LHC with an integrated luminosity (L) of 30 fb^{-1} and up to 1 TeV for $L = 300$ fb^{-1}.

1. Introduction

The Fermilab Tevatron Run II has been taking data since March 2001, and the CERN Large Hadron Collider (LHC) is planned to start running in Autumn 2009. One of the most important experimental goals of the Tevatron Run II and the LHC is the search for the mechanism of electroweak symmetry breaking—to discover the Higgs bosons or to prove their non-existence.

In the Standard Model, only one Higgs doublet is required to generate mass for both gauge bosons and elementary fermions, and the Higgs boson is the only particle remaining to be discovered in high energy experiments. In the minimal supersymmetric standard model (MSSM) [1], the Higgs sector has Yukawa interactions with two doublets, ϕ_1 and ϕ_2, whose neutral components couple to fermions with weak isospin $t_3 = -1/2$ and $t_3 = +1/2$ respectively [2]. After spontaneous symmetry breaking, there remain five physical Higgs bosons: a pair of singly charged Higgs bosons $H^{\pm}$, two neutral CP-even scalars H^0 (heavier) and h^0 (lighter), and a neutral CP-odd pseudoscalar A^0. The Higgs potential is constrained by supersymmetry such that all tree-level Higgs boson masses and couplings are determined by just two independent parameters, commonly chosen to be the mass of the CP-odd pseudoscalar (M_A) and the ratio of vacuum expectation values of neutral Higgs fields ($\tan\beta \equiv v_2/v_1$).

At the LHC, gluon fusion ($gg \to \phi^0$; $\phi^0 = h^0, H^0, A^0$) is the major source of neutral Higgs bosons in the MSSM for $\tan\beta$ less than 5. For $\tan\beta > 7$, neutral Higgs bosons are dominantly produced from bottom quark fusion $b\bar{b} \to \phi^0$ [3–7]. Since the Yukawa couplings of $\phi^0 b\bar{b}$ are enhanced by $1/\cos\beta$, the production rate of neutral Higgs bosons associated with bottom quarks, especially that of the A^0 or the H^0, is enhanced at large $\tan\beta$.

For a Higgs boson produced along with a single bottom quark at high transverse momentum (p_T), the leading-order subprocess is $bg \to b\phi^0$ [8–12]. If two high p_T bottom quarks are required in association with a Higgs boson, the leading order subprocess should be $gg \to b\bar{b}\phi$ [3,13–16]. In 2002, it was suggested that the search at the LHC for a Higgs boson produced along with a single bottom quark with large p_T should be more promising than the production of a Higgs boson associated with two high p_T bottom quarks [10]. This has already been shown to be the case for the $\mu^+\mu^-$ decay mode of the Higgs bosons [17].

For large $\tan\beta$, the $\tau^+\tau^-$ decay mode [18,19] can be a promising discovery channel for the A^0 and the H^0 in the MSSM. Recently, the discovery channel $b\phi^0 \to b\tau^+\tau^-$ has been demonstrated to offer great promise at the LHC to search for the A^0 and the H^0 up to $M_A = 1$ TeV [20].

The Higgs decay into $b\bar{b}$ has the largest branching fraction for large values of $\tan\beta$. However, the inclusive channel of $pp \to \phi^0 \to b\bar{b} + X$ is very challenging at the LHC owing to the extremely large QCD background. Previous theoretical studies have focused on the associated production of $b\bar{b}\phi^0 \to b\bar{b}b\bar{b}$ [21–23]. Realistic simulations by the ATLAS and the CMS Collaborations with parton showering lead to pessimistic results [24–26], because the trigger for the $4b$ final state requires high p_T bottom quarks for $pp \to b\bar{b}\phi^0 \to b\bar{b}b\bar{b} + X$. The requirement of four high p_T b-quarks removes most of the Higgs events. Moreover, integrating over the fourth b-quark to study a $3b$ signal requires a careful inclusion of higher order corrections in the four-flavor scheme. These poten-

* Corresponding author.
E-mail addresses: kao@physics.ou.edu (C. Kao), sayre@physics.ou.edu (J. Sayre).

0370-2693
doi:10.1016/j.physletb.2009.11.024

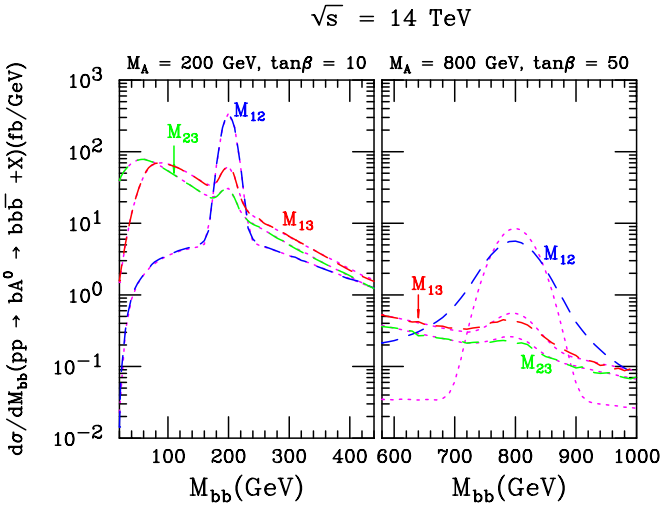

Fig. 1. The invariant-mass distribution of $b\bar{b}$ and bb pairs $d\sigma/dM_{b\bar{b}}(pp \to bb\bar{b} + X)$, for the Higgs signal from $bg \to bA^0$ with $M_A = 200$ GeV and $\tan\beta = 10$ as well as $M_A = 800$ GeV for $\tan\beta = 10$ and $\tan\beta = 50$. We calculate the Higgs signal with a Breit–Wigner resonance (dash) and in the narrow width approximation (dot), applying minimal cuts of $p_T > 10$ GeV and $|\eta| < 10$.

tially large leading-log corrections are absorbed into the b-quark PDFs in the five flavor scheme which we employ.

In this Letter, we present the prospects for discovering the MSSM neutral Higgs bosons produced with a single high p_T bottom quark (b or $\bar{b}$) followed by Higgs decay into a pair of bottom quarks. We calculate the Higgs signal and the dominant Standard Model (SM) backgrounds with exact matrix elements as well as realistic cuts and efficiencies. Furthermore, we present promising 5σ discovery contours at the LHC in the $(M_A, \tan\beta)$ plane. Section 2 shows the production cross sections and branching fractions for the Higgs signal. The SM physics background is discussed in Section 3. Sections 4 and 5 present the discovery potential at the LHC and the Fermilab Tevatron Run II. Optimistic conclusions are drawn in Section 6.

2. The production cross sections and branching fractions

At the LHC or the Tevatron Run II, the production cross section of $bg \to b\phi^0 \to bb\bar{b}$, where $\phi^0 = H^0, h^0, A^0$, is evaluated with the parton distribution functions of CTEQ6L1 [27] and the factorization scale $\mu_F = M_H/4$ [10]. In this Letter, b represents a bottom quark (b) or a bottom anti-quark ($\bar{b}$) unless it is explicitly specified. The bottom quark mass in the $\phi^0 b\bar{b}$ Yukawa coupling is chosen to be the next-to-leading-order (NLO) running mass $m_b(\mu_R)$ [28], which is calculated with $m_b(\text{pole}) = 4.7$ GeV and the NLO evolution of the strong coupling [29]. We have also taken the renormalization scale to be $M_H/4$. This choice of scale effectively reproduces the effects of next-to-leading order (NLO) corrections [10]. Therefore, we take the K factor to be one for the Higgs signal.

At the LHC, we calculate the Higgs cross section $\sigma(pp \to b\phi^0 \to bb\bar{b} + X)$ with a Breit–Wigner resonance via $bg \to b\phi^0 \to bb\bar{b}$. In addition, we check the cross section with the narrow width approximation

$$\sigma\left(pp \to b\phi^0 \to bb\bar{b} + X\right) = \sigma\left(pp \to b\phi^0 + X\right) \times B\left(\phi^0 \to b\bar{b}\right)$$

where $B(\phi^0 \to b\bar{b})$ is the branching fraction of a Higgs boson decay into $b\bar{b}$.

Fig. 1 shows the invariant-mass distribution (M_{ij}, $i, j = 1, 2, 3$) of the $b_i b_j$ or $b_i \bar{b}_j$ pairs for the Higgs signal $pp \to bA^0 \to bb\bar{b} + X$ via $bg \to bA^0$. The bottom quarks are ordered according to their transverse momenta, $p_T(b_1) \geqslant p_T(b_2) \geqslant p_T(b_3)$. We note that with energy-momentum smearing, the cross section in the narrow width approximation (NWA) agrees very well with that evaluated via a Breit–Wigner resonance (BWR) for most parameters that we have chosen. Based on the ATLAS [24] specifications, we model these effects by Gaussian smearing of momenta:

$$\frac{\Delta E}{E} = \frac{0.60}{\sqrt{E}} \oplus 0.03 \tag{1}$$

for jets at the LHC, with individual terms added in quadrature. For the Tevatron we use

$$\frac{\Delta E}{E} = \frac{0.50}{\sqrt{E}} \oplus 0.03 \tag{2}$$

based on CDF parameters [30]. For $M_A = 800$ GeV and $\tan\beta = 50$, the cross sections are in agreement within 10%. For large values of M_A, the increased width of the Higgs may lead to a reduced signal due to cuts on the dijet invariant-mass acceptance window. This effect is less well-modeled in the NWA than with BWR, although the total cross-sections remain in good agreement.

3. The physics background

The final state of $bb\bar{b}$ has dominant physics backgrounds coming from (a) $bg \to bb\bar{b}$, (b) $cg \to cb\bar{b}$, (c) $qg \to qb\bar{b}$ with $q = u, d, s$, (d) $q\bar{q} \to gb\bar{b}$ with $q = u, d, s, c$, and (e) $gg, q\bar{q} \to t\bar{t} \to b\bar{b}jj\ell\nu$, or $gg, q\bar{q} \to t\bar{t} \to b\bar{b}jjjj$. We have computed the cross section of the Higgs signal and physics background utilizing MadGraph [31,32] and HELAS [33] to generate matrix elements. To reduce the physics background while keeping most of the signal events, we require that in each event there are three jets (at least two b-jets) which satisfy the following requirements:

(a) we consider two sets of cuts for an integrated luminosity (L) of 30 fb^{-1} (low luminosity, LL): (i) $p_T(j_1) > 50$ GeV, $p_T(j_2) > 30$ GeV and $p_T(j_3) > 20$ GeV (low p_T cuts), or (ii) $p_T(j_1, j_2, j_3) > 70$ GeV (CMS 3-jet trigger) [26] as well as the pseudorapidity, $|\eta| < 2.5$ for all jets, where $p_T(j_1) > p_T(j_2) > p_T(j_3)$, or

(b) for $L = 300$ fb^{-1} (high luminosity, HL) we check two sets of cuts: (i) $p_T(j_1, j_2, j_3) > 75$ GeV (ATLAS 3-jet trigger) [25] or (ii) $p_T(j_1, j_2, j_3) > 150$ GeV (ATLAS 3-jet trigger for high luminosity) [25] as well as $|\eta| < 2.5$ for all jets,

(c) there is at least one pair of bottom quarks in the Higgs mass window such that $|M_{bb} - M_\phi| < \Delta M_{bb}$, where $\Delta M_{bb} = \text{MAX}(22\text{ GeV}, \sigma_M)$, choosing $\sigma_M = 0.10 \times M_\phi$ or $0.15 \times M_\phi$ for $L = 30$ fb^{-1} and $\sigma_M = 0.15 \times M_\phi$ or $0.20 \times M_\phi$ for $L = 300$ fb^{-1},

(d) all three jets are separated with $\Delta R = \sqrt{\Delta\phi^2 + \Delta\eta^2} > 0.7$ (where ϕ is the angle between two jets in the transverse plane),

(e) the missing transverse energy ($\not{E}_T$) should be less than 40 GeV.

In addition, we veto events with more than three jets passing the cuts $p_T(j) > 15$ GeV and $|\eta| < 2.5$. We take the b-tagging efficiency to be $\epsilon_b = 0.6$ (LL) or $\epsilon_b = 0.5$ (HL), the probability that charm quark may be misidentified is $\epsilon_c = 0.15$, and the probability that a light quark or a gluon may be misidentified as a bottom quark is $\epsilon_j = 0.01$. For the backgrounds arising from $bb\bar{b}$ and $jb\bar{b}$ [21] as well as those from $t\bar{t}$ [34], we assume a K factor of 2 when computing the significance as discussed below. In practice we find that the $t\bar{t}$ backgrounds are negligible after cuts, although we include them for completeness.

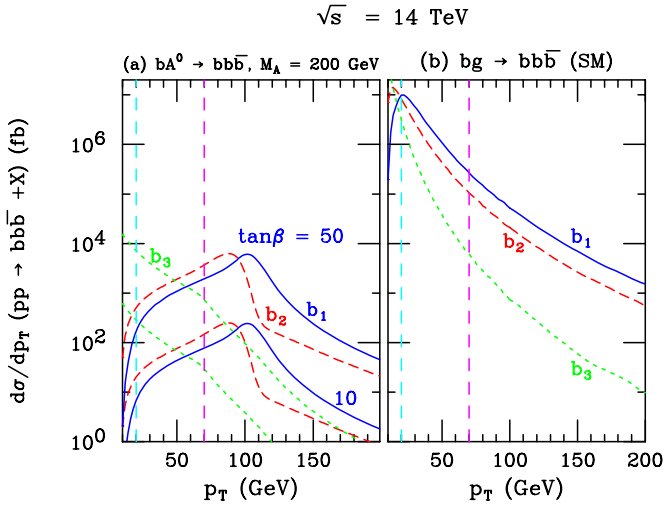

Fig. 2. The transverse-momentum distribution for (a) the Higgs signal from $bg \to bA^0$ with $M_A = 200$ GeV and $\tan\beta = 10, 50$ as well as for (b) the physics background from $bg \to bb\bar{b}$. We require $p_T(b) > 10$ GeV and $|\eta_b| < 2.5$ in this figure. The vertical, dashed lines illustrate cuts at 20 GeV and 70 GeV.

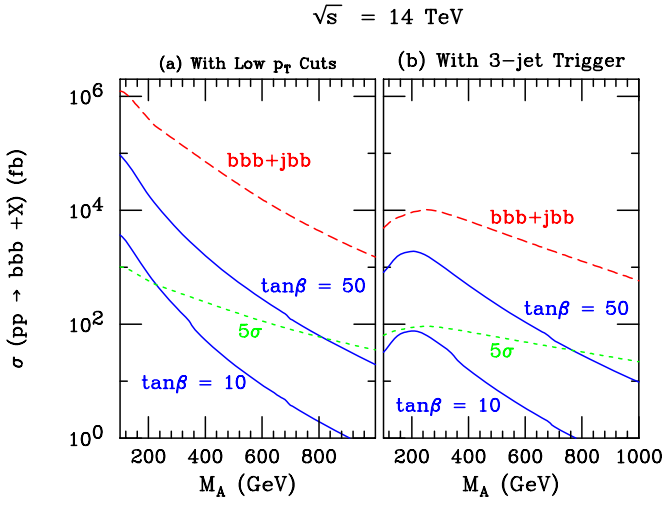

Fig. 3. The signal cross section of $bg \to bA^0$ at the LHC for an integrated luminosity $L = 30$ fb^{-1}, as a function of M_A, for $m_{\tilde{q}} = m_{\tilde{g}} = \mu = 1$ TeV, $\tan\beta = 10$ and $\tan\beta = 50$. Also shown are the background cross sections in the mass window of $M_A \pm 0.10 \times M_A$ as discussed in the text for the SM contributions. We have applied acceptance cuts and efficiencies of tagging and mistagging.

In Fig. 2, we present the transverse-momentum distribution $(d\sigma/dp_T)$ of the bottom quarks (b or $\bar{b}$), for the Higgs signal $pp \to bA^0 \to bb\bar{b} + X$. Also shown is the p_T distribution for bottom quarks from the SM background $bg \to bb\bar{b}$. We have required $p_T(b) > 10$ GeV and $|\eta_b| < 2.5$ in this figure.

4. The discovery potential at the LHC

To study the discovery potential of $pp \to b\phi^0 \to bb\bar{b} + X$ ($\phi^0 = H^0, h^0, A^0$) at the LHC, we calculate the Higgs signal as well as the SM physics background in the mass window of $M_\phi \pm \Delta M_{bb}$ where $\Delta M_{bb} = \text{MAX}(22\text{ GeV}, 0.10 \times M_\phi)$, or $\Delta M_{bb} = \text{MAX}(22\text{ GeV}, 0.15 \times M_\phi)$ for an integrated luminosity of 30 fb^{-1}.

In Fig. 3 we show the cross section of $\sigma(pp \to bA^0 \to bb\bar{b} + X)$, for $\tan\beta = 10$ and 50, with a common mass for scalar quarks, scalar leptons and the gluino $m_{\tilde{f}} = m_{\tilde{g}} = \mu = 1$ TeV. We also present the background cross sections with no K factor in the mass window of $M_A \pm \Delta M_{bb}$ for the dominant SM processes $pp \to bb\bar{b} + X$ and $pp \to jb\bar{b} + X$, $j = q, \bar{q}, g$, with (a) low p_T cuts and (b) CMS 3-jet trigger. The cuts and tagging efficiencies are included with $\Delta M_{bb} = 0.10 \times M_A$. In addition, we present the 5σ cross section for $L = 30$ fb^{-1}. The cross section of the Higgs signal with $\tan\beta \simeq 50$ can be larger than the 5σ cross section for $M_A \lesssim 800$ after acceptance cuts. Requiring higher transverse momenta ($p_T > 70$ GeV) greatly reduces the background and the Higgs signal for $M_A < 200$ GeV.

We define the signal to be observable if the lower limit on the signal plus background is larger than the corresponding upper limit on the background [35,36], namely,

$$L(\sigma_s + \sigma_b) - N\sqrt{L(\sigma_s + \sigma_b)} > L\sigma_b + N\sqrt{L\sigma_b} \tag{3}$$

which corresponds to

$$\sigma_s > \frac{N^2}{L}[1 + 2\sqrt{L\sigma_b}/N]. \tag{4}$$

Here L is the integrated luminosity, σ_s is the cross section of the Higgs signal, and σ_b is the background cross section. Both cross sections are taken to be within a bin of width $\pm\Delta M_{bb}$ centered at M_ϕ. In this convention, $N = 2.5$ corresponds to a 5σ signal. We take the integrated luminosity L to be 30 fb^{-1} and 300 fb^{-1} [24].

For $\tan\beta \gtrsim 10$, M_A and M_H are almost degenerate when $M_A \gtrsim 125$ GeV, while M_A and m_h are very close to each other for $M_A \lesssim 125$ GeV in the MSSM [37]. Therefore, when computing the discovery reach, we add the cross sections of the A^0 and the h^0 for $M_A < 125$ GeV and those of the A^0 and the H^0 for $M_A \geqslant 125$ GeV [24,26,38].

Fig. 4 shows the 5σ discovery contours for the MSSM Higgs bosons where the discovery region is the part of the parameter space above the contour. We have chosen $M_{\text{SUSY}} = m_{\tilde{q}} = m_{\tilde{g}} = m_{\tilde{\ell}} = \mu = 1$ TeV. If M_{SUSY} is smaller, the discovery region of $A^0, H^0 \to b\bar{b}$ will be slightly reduced for $M_A \gtrsim 250$ GeV, because the Higgs bosons can decay into supersymmetric (SUSY) particles [39] and the branching fraction of $\phi^0 \to b\bar{b}$ is suppressed. For $M_A \lesssim 125$ GeV, the discovery region of $H^0 \to b\bar{b}$ is slightly enlarged for a smaller M_{SUSY}, but the observable region of $h^0 \to b\bar{b}$ is slightly reduced because the lighter top squarks make the H^0 and the h^0 lighter; also the $H^0 b\bar{b}$ coupling is enhanced while the $h^0 b\bar{b}$ coupling is reduced [38].

In addition, we have studied the effect of an invariant-mass cut, using only the two jets with highest p_T as the candidate pair. Table 1 presents the cross section corresponding to two schemes: (a) requiring $|M_{12} - M_\phi| < \Delta M_{bb}$, and (b) requiring $|M_{ij} - M_\phi| < \Delta M_{bb}$; $i, j = 1, 2, 3$. We find that for $M_A \gtrsim 400$, it is more advantageous to apply an invariant-mass cut only on the two leading b jets. For lower masses using any pair of the three leading jets leads to higher significance. We also show the ratio of signal to background in this figure. We have chosen a set of cuts, $p_T(j_1, j_2, j_3) > 100, 80, 70$ GeV, which tends to maximize this ratio. Less stringent cuts can improve the nominal statistical significance in the low mass regions, but for high masses and low $\tan\beta$ the small signal to background ratio would require excellent understanding of backgrounds and systematic errors.

Furthermore, we have studied the effects of SUSY particles on the $\phi^0 b\bar{b}$ Yukawa couplings at large $\tan\beta$. The SUSY contributions can be described with an effective Lagrangian and a function Δ_b [40–43] such that the bottom quark mass in Yukawa couplings becomes

$$m_b \to \frac{m_b}{1 + \Delta_b}$$

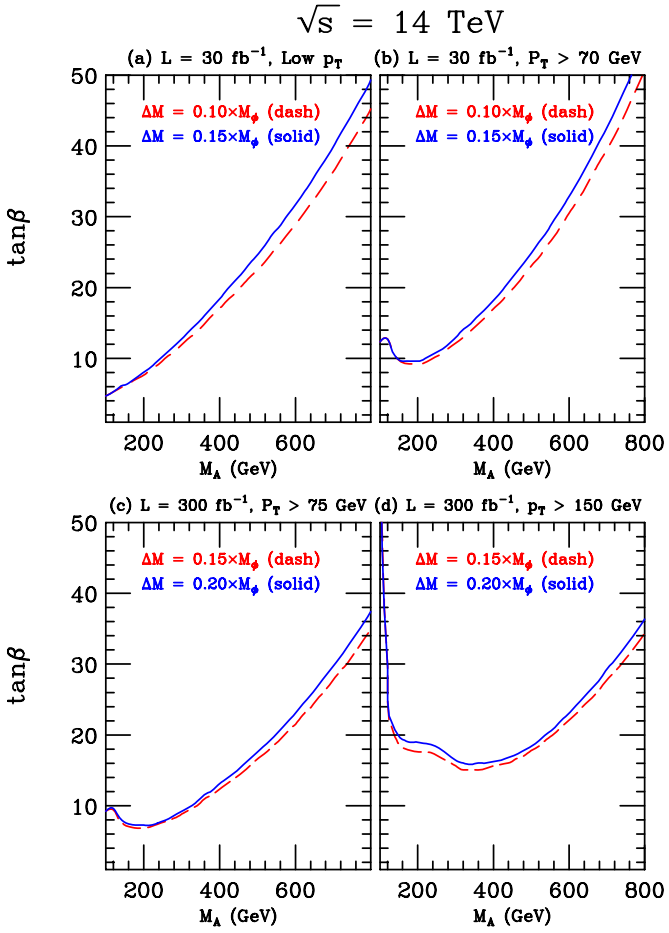

Fig. 4. The 5σ discovery contours at the LHC with $\sqrt{s} = 14$ TeV for (a) $L = 30$ fb^{-1} and low p_T cuts, (b) $L = 30$ fb^{-1} and $p_T > 70$ GeV, (c) $L = 300$ fb^{-1} and $p_T > 75$ GeV, (d) $L = 300$ fb^{-1} and $p_T > 150$ GeV, in the M_A versus $\tan\beta$ plane. The signal includes $\phi^0 = A^0$ and h^0 for $M_A < 125$ GeV, and $\phi^0 = A^0$ and H^0 for $M_A \geqslant 125$ GeV. The discovery region is the part of the parameter space above the contours.

where SUSY QCD corrections lead to

$$\Delta_b = \Delta_b^{\tilde{b}} = \frac{2\alpha_s}{3\pi} m_{\tilde{g}} \mu \tan\beta I(m_{\tilde{b}_1}, m_{\tilde{b}_2}, m_{\tilde{g}})$$

for bottom squarks and gluinos, and the auxiliary function is

$$I(a,b,c) = -\frac{1}{(a^2-b^2)(b^2-c^2)(c^2-a^2)} \times \left(a^2 b^2 \ln\frac{a^2}{b^2} + b^2 c^2 \ln\frac{b^2}{c^2} + c^2 a^2 \ln\frac{c^2}{a^2}\right).$$

Then the cross section can be estimated with a simple formula [43]

$$\sigma\left(pp \to b\phi^0 + X\right) \times B\left(\phi^0 \to b\bar{b}\right) \simeq \sigma_{SM}(pp \to bH + X) \times \frac{\tan^2\beta}{(1+\Delta_b)^2} \times \frac{9}{(1+\Delta_b)^2 + 9}.$$

In our analysis of SUSY effects, we adopt the conventions in Refs. [12,44] and have used a more complete estimate, including the effects of the modified Higgs width in the full BWR calculation. Table 2 shows the cross section including (a) no SUSY effects, (b) contributions from bottom squarks and gluinos, and (c) contributions from bottom squarks and gluinos as well as from top squarks and Higgsinos. The top squark/Higgsino loops give an additional effective correction to m_b,

$$\Delta_b^{\tilde{t}} = \frac{\alpha_t}{4\pi} A_t \mu \tan\beta I(m_{\tilde{t}_1}, m_{\tilde{t}_2}, \mu),$$

where $\alpha_t \equiv \lambda_t^2/4\pi$ ($\lambda_t = \sqrt{2} m_t/v_2$ being the top Yukawa coupling), and A_t is the trilinear Higgs-stop coupling. It is clear that SUSY effects reduce the Higgs cross section for a positive μ while they enhance the Higgs cross section for a negative μ. The effect of the Higgsino/stop loops is highly dependant on the size of A_t. We present two scenarios, M_h^{max} and no-mixing, as defined in Ref. [43]. In the former the Higgsino/stop contribution is comparable to the gluino/bottom-squark term, in the latter it is almost negligible.

Table 1
Cross sections in fb for the Higgs signal and physics background for two choices of cuts on the invariant mass of $b\bar{b}$: (a) two leading jets (M_{12}) versus (b) any two jets (M_{ij}) used to reconstruct the Higgs invariant mass. Significances are computed with $L = 30$ fb^{-1}.

Mass (GeV)		Signal	Background	Significance ($N_{SS} = N_S/\sqrt{N_B + N_S}$)	N_S/N_B
			$\tan\beta = 10$		
200	M_{12}	44.2	3960	3.82	1.12×10^{-2}
	M_{ij}	126	14500	5.72	8.70×10^{-3}
400	M_{12}	23.5	6680	1.57	3.52×10^{-3}
	M_{ij}	32.2	11900	1.61	2.70×10^{-3}
800	M_{12}	1.42	1400	0.208	1.02×10^{-3}
	M_{ij}	1.61	2380	0.181	6.76×10^{-4}
			$\tan\beta = 20$		
200	M_{12}	178	3960	15.1	4.48×10^{-2}
	M_{ij}	498	14500	22.2	3.43×10^{-2}
400	M_{12}	104	6680	6.94	1.56×10^{-2}
	M_{ij}	143	11900	7.14	1.20×10^{-2}
800	M_{12}	6.99	1400	1.02	5.00×10^{-3}
	M_{ij}	7.96	2380	0.891	3.34×10^{-3}
			$\tan\beta = 50$		
200	M_{12}	961	3960	75.0	2.42×10^{-1}
	M_{ij}	2770	14500	115	1.91×10^{-1}
400	M_{12}	563	6680	36.2	8.43×10^{-2}
	M_{ij}	792	11900	38.5	6.66×10^{-2}
800	M_{12}	38.7	1400	5.58	2.76×10^{-2}
	M_{ij}	44.7	2380	4.96	1.87×10^{-2}

Table 2
Effect of Δ_b in M_h^{max} (no mixing) scenario. Cross sections in fb for $pp \to b\phi^0 \to b\bar{b}b\bar{b} + X$ using high p_T (> 70 GeV) cuts. Tagging efficiencies have not been applied.

Mass (GeV)		$\Delta_b = 0$	$\tilde{g}/\tilde{b}$	$\tilde{g}/\tilde{b} + \tilde{H}/\tilde{t}$
		$\tan\beta = 10$		
200	$\mu = +200$	698(708)	646(658)	633(656)
	$\mu = -200$	699(703)	745(755)	761(753)
400	$\mu = +200$	155(155)	143(144)	140(145)
	$\mu = -200$	156(155)	168(167)	172(168)
800	$\mu = +200$	7.90(7.91)	7.28(7.31)	7.07(7.31)
	$\mu = -200$	7.87(7.93)	8.63(8.56)	8.86(8.60)
		$\tan\beta = 50$		
200	$\mu = +200$	16400(16400)	12200(12200)	11000(12200)
	$\mu = -200$	16400(16300)	22600(22600)	25800(22600)
400	$\mu = +200$	4120(4120)	3060(3060)	2750(3060)
	$\mu = -200$	4130(4120)	5730(5730)	6560(5720)
800	$\mu = +200$	233(233)	172(172)	154(172)
	$\mu = -200$	233(233)	325(325)	373(325)

5. The discovery potential at the Fermilab Tevatron

To study the discovery potential of Higgs decays into bottom quark pairs at the Fermilab Tevatron Run II, we require:

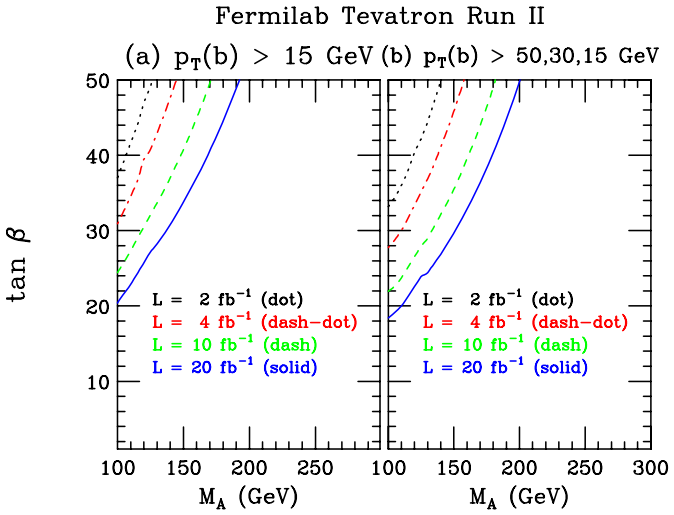

Fig. 5. The 5σ discovery contours at the Fermilab Tevatron Run II for an integrated luminosity (L) of 4 fb^{-1}, 10 fb^{-1}, 20 fb^{-1} in the M_A versus $\tan\beta$ plane. The signal includes $\phi^0 = A^0$ and h^0 for $M_A < 125$ GeV, and $\phi^0 = A^0$ and H^0 for $M_A \geqslant 125$ GeV. The discovery region is the part of the parameter space above the contours.

(i) three b quarks or 3 jets (at least two b jets) with $p_T > 15$ GeV or $p_T(j_1, j_2, j_3) > 50, 30, 15$ GeV, $|\eta(b, j)| < 2.0$, and a b-tagging efficiency $\epsilon_b = 50\%$ [30],
(ii) the angular separation between each pair of jets should be $\Delta R > 0.4$ [45],
(iii) the invariant mass of the reconstructed bottom quark pairs should be within the mass window of the Higgs mass with $\Delta M_{bb} = \text{MAX}(0.1 \times M_\phi, 20\ \text{GeV})$.

Fig. 5 show the 5σ discovery contours for the MSSM Higgs bosons, where the discovery region is the part of the parameter space above the curves. The discovery contours for $\Delta M_{bb} = 0.10 \times M_\phi$ [46] are comparable to those presented in this figure.

We find that the Tevatron Run II can discover neutral Higgs bosons in the MSSM for a value of $\tan\beta$ slightly less than 30 with an integrated luminosity of 4 fb^{-1} and $M_A < 120$ GeV. For $\tan\beta \sim 50$, the Tevatron Run II will be able to discovery the Higgs bosons up to $M_A \sim 160$ GeV with $L = 4$ fb^{-1}, and up to $M_A \sim 200$ GeV with $L = 20$ fb^{-1}. Our results are consistent with those found in Refs. [23,45,47].

6. Conclusions

The associated production of a Higgs boson with a bottom quark, followed by the Higgs decay into bottom quark pairs, is a promising channel for the discovery of the neutral Higgs bosons in the minimal supersymmetric standard model at the LHC. The A^0 and the H^0 should be observable in a large region of parameter space with $\tan\beta \gtrsim 10$. The associated final state of $b\phi^0 \to bb\bar{b}$ could discover the A^0 and the H^0 at the LHC with an integrated luminosity of 30 fb^{-1} if $M_A \lesssim 800$ GeV. At a higher luminosity of 300 fb^{-1}, the discovery region in M_A is expanded up to $M_A = 1$ TeV for $\tan\beta \sim 50$.

In our analysis, we apply a mass cut, requiring the reconstructed Higgs mass to lie in the mass window $M_\phi \pm \Delta M_{bb}$. We note that improvements in the discovery potential will be possible by narrowing ΔM_{bb} if the bottom quark pair mass resolution can be improved. In regions of high mass and low $\tan\beta$ the ratio of signal to background events is very low. Discovery in these regions would require either excellent understanding of backgrounds in order to lower systematic errors below the few percent level, or better discrimination between signal and background due to narrower ΔM_{bb} or improved b-tagging. Our results using three b's are more promising than those found in previous studies based on $4b$ analyses [21,22,25,26].

The discovery of the associated final state of $b\phi^0 \to bb\bar{b}$ along with $b\phi^0 \to b\tau^+\tau^-$ [20] and $b\phi \to b\mu^+\mu^-$ [17] will provide information about the Yukawa couplings of $f\bar{f}\phi^0$; $f = b, \tau, \mu$, for fermions with $t_3 = -1/2$. Furthermore, the muon pair channel can also be observable in a significantly large region and the muon pair channel will provide a good opportunity to precisely reconstruct the masses for MSSM Higgs bosons [13,17,38]. In concert, this family of channels may provide an excellent window on the Yukawa sector of the MSSM.

Acknowledgements

We are grateful to Michelangelo Mangano for beneficial instruction and discussions. C.K. thanks the Physics Division of CERN for hospitality and support during a sabbatical visit. This research was supported in part by the U.S. Department of Energy under Grant No. DE-FG02-04ER41305.

References

[1] H.P. Nilles, Phys. Rep. 110 (1984) 1;
H.E. Haber, G.L. Kane, Phys. Rep. 117 (1985) 75.
[2] J. Gunion, H. Haber, G. Kane, S. Dawson, The Higgs Hunter's Guide, Addison–Wesley, Redwood City, CA, 1990.
[3] D.A. Dicus, S. Willenbrock, Phys. Rev. D 39 (1989) 751.
[4] D. Dicus, T. Stelzer, Z. Sullivan, S. Willenbrock, Phys. Rev. D 59 (1999) 094016.
[5] C. Balazs, H.J. He, C.P. Yuan, Phys. Rev. D 60 (1999) 114001.
[6] F. Maltoni, Z. Sullivan, S. Willenbrock, Phys. Rev. D 67 (2003) 093005.
[7] R.V. Harlander, W.B. Kilgore, Phys. Rev. D 68 (2003) 013001.
[8] D. Choudhury, A. Datta, S. Raychaudhuri, arXiv:hep-ph/9809552.
[9] C.S. Huang, S.H. Zhu, Phys. Rev. D 60 (1999) 075012.
[10] J. Campbell, R.K. Ellis, F. Maltoni, S. Willenbrock, Phys. Rev. D 67 (2003) 095002.
[11] J.J. Cao, G.P. Gao, R.J. Oakes, J.M. Yang, Phys. Rev. D 68 (2003) 075012.
[12] S. Dawson, C.B. Jackson, Phys. Rev. D 77 (2008) 015019.
[13] S. Dawson, D. Dicus, C. Kao, Phys. Lett. B 545 (2002) 132.
[14] B. Plumper, DESY-THESIS-2002-005.
[15] S. Dittmaier, M.I. Kramer, M. Spira, Phys. Rev. D 70 (2004) 074010.
[16] S. Dawson, C.B. Jackson, L. Reina, D. Wackeroth, Phys. Rev. D 69 (2004) 074027.
[17] S. Dawson, D. Dicus, C. Kao, R. Malhotra, Phys. Rev. Lett. 92 (2004) 241801.
[18] Z. Kunszt, F. Zwirner, Nucl. Phys. B 385 (1992) 3.
[19] E. Richter-Was, D. Froidevaux, F. Gianotti, L. Poggioli, D. Cavalli, S. Resconi, Int. J. Mod. Phys. A 13 (1998) 1371.
[20] C. Kao, D.A. Dicus, R. Malhotra, Y. Wang, Phys. Rev. D 77 (2008) 095002.
[21] J. Dai, J.F. Gunion, R. Vega, Phys. Lett. B 345 (1995) 29;
Phys. Lett. B 387 (1996) 801.
[22] J.L. Diaz-Cruz, H.J. He, T.M.P. Tait, C.P. Yuan, Phys. Rev. Lett. 80 (1998) 4641;
C. Balazs, J.L. Diaz-Cruz, H.J. He, T.M.P. Tait, C.P. Yuan, Phys. Rev. D 59 (1999) 055016.
[23] M.S. Carena, S. Mrenna, C.E.M. Wagner, Phys. Rev. D 60 (1999) 075010.
[24] G. Aad, et al., ATLAS Collaboration, Expected Performance of the ATLAS Experiment – Detector, Trigger and Physics, arXiv:0901.0512 [hep-ex], 2009.
[25] K. Mahboubi, ATLAS level-1 jet trigger rates and study of the ATLAS discovery potential of the neutral MSSM Higgs bosons in b-jet decay channels, Ph.D. thesis, Heidelberg U., 2001.
[26] G.L. Bayatian, et al., CMS Collaboration, J. Phys. G 34 (2007) 995.
[27] J. Pumplin, D.R. Stump, J. Huston, H.L. Lai, P. Nadolsky, W.K. Tung, JHEP 0207 (2002) 012.
[28] J.A.M. Vermaseren, S.A. Larin, T. van Ritbergen, Phys. Lett. B 405 (1997) 327.
[29] W.J. Marciano, Phys. Rev. D 29 (1984) 580.
[30] A. Abulencia, et al., CDF Collaboration, Phys. Rev. D 73 (2006) 032003.
[31] MADGRAPH, by T. Stelzer, W.F. Long, Comput. Phys. Commun. 81 (1994) 357.
[32] F. Maltoni, T. Stelzer, JHEP 0302 (2003) 027.
[33] HELAS, by H. Murayama, I. Watanabe, K. Hagiwara, KEK report KEK-91-11, 1992.
[34] R. Bonciani, S. Catani, M.L. Mangano, P. Nason, Nucl. Phys. B 529 (1998) 424;
P. Nason, S. Dawson, R.K. Ellis, Nucl. Phys. B 303 (1988) 607.
[35] H. Baer, M. Bisset, C. Kao, X. Tata, Phys. Rev. D 46 (1992) 1067.

[36] N. Brown, Z. Phys. C 49 (1991) 657.
[37] M. Carena, J.R. Espinosa, M. Quiros, C.E.M. Wagner, Phys. Lett. B 355 (1995) 209;
S. Heinemeyer, W. Hollik, G. Weiglein, Phys. Rev. D 58 (1998) 091701; and references therein.
[38] C. Kao, N. Stepanov, Phys. Rev. D 52 (1995) 5025.
[39] H. Baer, M. Bisset, D. Dicus, C. Kao, X. Tata, Phys. Rev. D 47 (1993) 1062;
H. Baer, M. Bisset, C. Kao, X. Tata, Phys. Rev. D 50 (1994) 316.
[40] L.J. Hall, R. Rattazzi, U. Sarid, Phys. Rev. D 50 (1994) 7048.
[41] M.S. Carena, M. Olechowski, S. Pokorski, C.E.M. Wagner, Nucl. Phys. B 426 (1994) 269.
[42] D.M. Pierce, J.A. Bagger, K.T. Matchev, R.j. Zhang, Nucl. Phys. B 491 (1997) 3.
[43] M.S. Carena, S. Heinemeyer, C.E.M. Wagner, G. Weiglein, Eur. Phys. J. C 45 (2006) 797.
[44] S. Dawson, C. Kao, Y. Wang, Phys. Rev. D 77 (2008) 113005.
[45] CDF Collaboration, CDF note 9284, 2008, http://www-cdf.fnal.gov.
[46] U. Aglietti, et al., arXiv:hep-ph/0612172.
[47] P. Draper, T. Liu, C.E.M. Wagner, Phys. Rev. D 80 (2009) 035025.